

Supplementary Material

Data

Seismic data consisted of a 3D seismic survey covering ~2000 km² of the NE Faroe-Shetland Basin, provided by TGS.

This study utilises free-air gravity anomaly data (shown in Figs 1b and DR4), which is part of Getech's Multi-Satellite Gravity Data project, publicly available from the Oil and Gas Authority. The dataset is a composite of five overlapping gravity surveys collected by satellites (two in the 1980s, three completed by Getech in 2016). These satellites have varying orbital inclinations, so that the combined dataset has effective orbital spacing of <2 km at the equator, and a resolution of sub-5 km half-wavelength.

Methods

Seismic Interpretation

Seismic interpretation for this study was undertaken using Schlumberger Petrel software.

Horizons and sills were interpreted based on their seismic characteristics (Planke *et al.* 2000, 2015; Schofield *et al.* 2012, 2015; Mark *et al.* 2018) and interpolated to create continuous 3D surfaces. Top Basalt is typically characterised by a high-amplitude, largely continuous, positive reflection; while Base Basalt, which is constrained by well data, is characterised by a variable- (commonly low) amplitude negative reflection, often immediately underlain by intrusions (Fig. 2). Owing to the complex and transitional nature of the base of the volcanic sequence (Abdelmalak *et al.* 2016) it does not always produce a distinct reflection; in this case its position is estimated using the shallowest appearance of intrusions. The top and base of the volcanic sequence was interpreted using a grid spacing of ~300 m and ~600 m, respectively. To highlight geomorphological features of the volcanic

edifice the Top Basalt surface is displayed using RMS amplitude (extracted over a window of 30 ms; Fig. 1 and DR1).

More than 300 sills were interpreted within the sedimentary section beneath the extrusive basalt sequence, which are typically characterised by high-amplitude saucer-shaped or semi-saucer-shaped reflections that are locally transgressive (Schofield *et al.* 2012, 2015). These were interpreted using a combination of 3D autotrack and manual picking on a ~60 m grid spacing. The vertical resolution of the seismic data within this stratigraphic interval is around ~30 m, meaning that sills with a thickness less than this are not easily resolved (Mark *et al.* 2018), and there are therefore likely to be many more than the 300 interpreted intrusions. In addition, since steeply-dipping features are typically very poorly imaged on seismic data, it is probable that there are numerous unobserved dyke intrusions in addition to the sills beneath the volcanic edifice.

The top of the laccolithic complex is characterised by a high-amplitude positive reflection, which in many places has a stepped geometry, stepping downwards away from the pluton crest. This was interpreted using a grid spacing of ~600 m. Although the base of the complex is not clear, it is likely to be close to the lower high-amplitude reflection shown in DR2, and has been picked on the negative reflection just below (since high-velocity gabbro is overlying lower-velocity sedimentary rocks, this should result in a negative reflection). The base of the laccolith was interpreted using a grid spacing of ~1 km. For the purposes of imaging (Fig. 3B, DR1) the Top Laccolith surface is displayed using an RMS Amplitude extraction, taken over a window of 30 ms.

Gravity Modelling

In order to determine the most likely geometry and nature of the laccolithic complex underlying the Erlend volcano, the gravity responses of three different possibilities were

modelling, which were then compared with the observed free-air gravity anomaly. Several steps were involved in the modelling process, For simplicity, the gravity was modelling only along a single 2D line across the Erlend volcano rather than a 3D volume.

Firstly the seismic data (which was interpreted in TWT) was converted into depth using a velocity model constructed from interval velocities from nearby wells. The resulting depth-converted geological surfaces were then used as a basis for the gravity models.

The densities of the various stratigraphic units were then estimated using density logs from several nearby wells, and also theoretical estimates. Combining these densities with the thicknesses of the units (delineated by surfaces interpreted from the seismic data) allows the likely gravity signature above the volcano to be calculated (using the ARK CLS XField plugin for Schlumberger Petrel), which was then compared with the observed free-air gravity anomaly.

These steps are discussed in more detail in the following sections.

Depth Conversion

In order to create 2D gravity models, a 2D seismic line was converted from time into depth using interval velocities between interpreted horizons (DR6).

Interval velocities for the seawater column; Eocene-Recent and intruded Cretaceous sedimentary sections; and the extrusive basalts were taken from 209/03-1. The interval velocity for the sub-Cretaceous basement was calculated from the average sonic transit time within the basement from 209/09-1. The laccolith has not been penetrated by any wells, so an interval velocity was estimated based on experimental velocities for gabbro (Christensen & Mooney 1995).

Note that for Model A the volume of the ring dykes is extremely minor compared to the sedimentary portion of the Cretaceous section, and the dykes can therefore be assumed to have a correspondingly minor contribution to the interval velocity. For simplicity, it was decided to effectively ignore the contribution of the dykes to the velocity model, since they would barely affect the overall interval velocity (DR6). This is especially true since the Cretaceous section in 209/03-1 contains numerous intrusions, so the modelled interval velocity already accounts for the occurrence of intrusions within the mudstones.

Rock Densities

The density of the mafic ring dykes/lacoloth was calculated to be 2.99 g/cc based on the geochemistry of the Erlend lavas, which agrees closely with densities previously reported for gabbro (Washington 1917, p 1050-1063; Carmichael 1989; Christensen & Mooney 1995). Although acidic intrusions are present in the Erlend wells, their geochemistry indicates that they were generated by partial melting of country rock (Kanaris-Sotiriou *et al.* 1993). This, combined with the common occurrence of mafic sills in the wells, suggests that the modelled intrusive body is likely to be mafic rather than evolved, supporting the use of a gabbroic density for modelling.

The average densities from several nearby wells were used for the post-volcanic sedimentary section, extrusive basalts, sub-volcanic sedimentary section and pre-Cretaceous crystalline basement (Fig. 4; Table 1).

Notes for Table 1:

* The Erlend wells contain mixtures of tabular and compound lavas and hyaloclastites within the extrusive section, which each have different average densities. Since the bulk of the edifice comprises compound lava flows, only the densities for the compound flow intervals are included here.

** Within these wells, the Cretaceous section contains varying numbers of igneous (mainly mafic) intrusions. The densities in this table are an average across the entire Cretaceous section, and thus include contributions from both the sedimentary strata and the intrusions. Using this average density value allows us to simply account for the presence of numerous intrusions within the Cretaceous beneath the Erlend edifice. An alternative would be to determine the densities of the sedimentary strata and the intrusions separately, and then estimate their relative proportions to calculate an average value for the Cretaceous section. However, given that it is extremely difficult to estimate the proportion of igneous material with any precision due to the resolution limits of seismic data, this method would introduce extreme uncertainty into the gravity models.

Well	Average Interval Density (g/cc)			
	Eocene	Extrusive Basalt*	Cretaceous**	Basement
209/03-1		2.43	2.44	
209/04-1A	1.88	2.65	2.41	
209/06-1			2.46	
209/09-1	1.81	2.47	2.31	2.66
209/12-1				2.68
219/28-2Z			2.50	2.64
Average	1.84	2.51	2.42	2.66

Table 1: Densities taken from wells in the vicinity of Erlend for use in gravity modelling

Gravity Modelling

2D gravity modelling was undertaken using the ARK CLS XField plugin for Schlumberger Petrel. To reduce edge effects and account for the influence of bodies perpendicular to the 2D model, most of the model was assumed to extend laterally to infinity. The intrusive body

(or bodies) was assumed to extend for 7000 m perpendicular to the model (approximately the radius of the mapped dome).

The only variable changed between the models was the geometry of the intrusive body (or bodies) forming the domal reflection, which is based on seismic interpretation; all other parameters were identical. Note that, although the depth conversion for Model A results in a shallower depth and different geometry of the top of the basement compared with the other models (DR6), we have kept the depth and geometry of the basement consistent for the purposes of gravity modelling (Fig. 4). This enables us to test the sensitivity of the gravity models to variations in the intrusive body, rather than variations in the basement.

Video DR1 (G47941_SuppVid.mp4): Video showing the Erlend plumbing system rotating in 3D. The first part of the video shows the extrusive edifice, which fades to show the subjacent laccolith, radial sill network and conduit sill network.

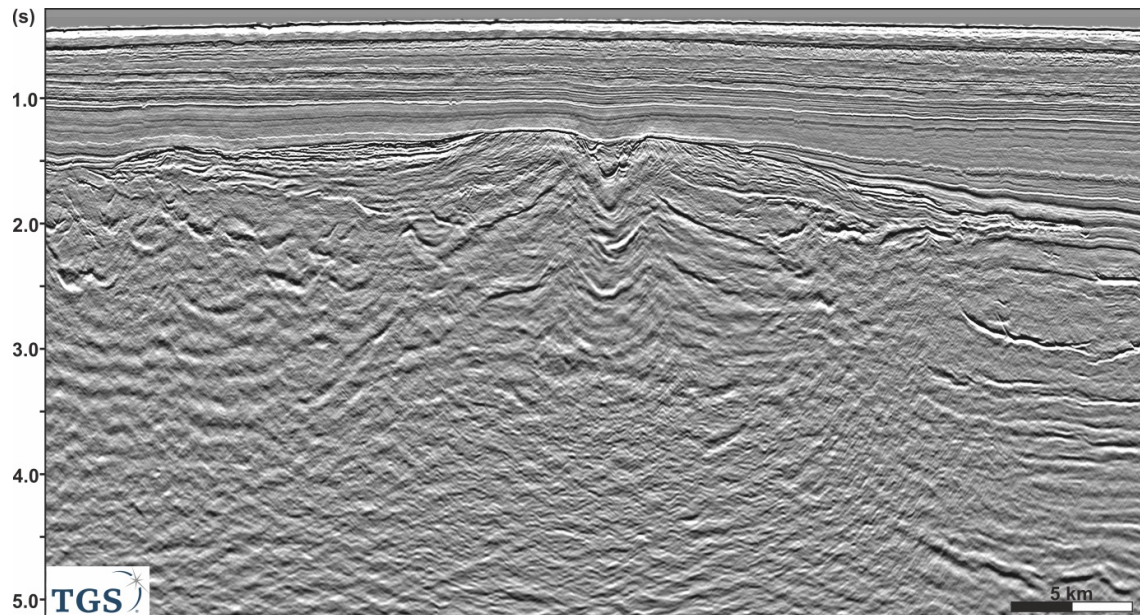


Fig. DR2: Uninterpreted arbitrary seismic line across the Erlend Volcano. For the interpreted version see Figure 2 in the main text. Line location shown in Figure 1b in the main text.

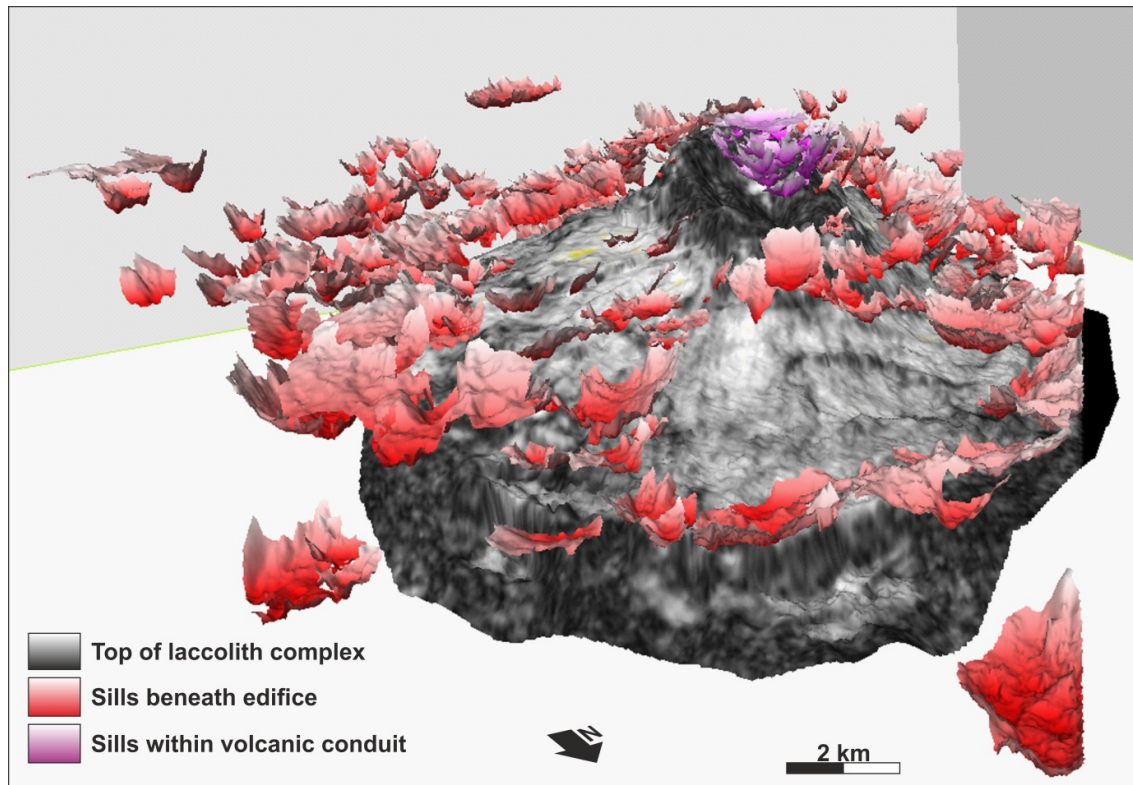


Fig. DR3: 3D view of the Erlend plumbing system, showing the top of the laccolith complex in B&W, sub-edifice sills in red, and conduit sills in purple. Note that many of the intrusions lack the saucer-shape common to sills, and have lower margins that appear to terminate at or close to the top of the laccolith.

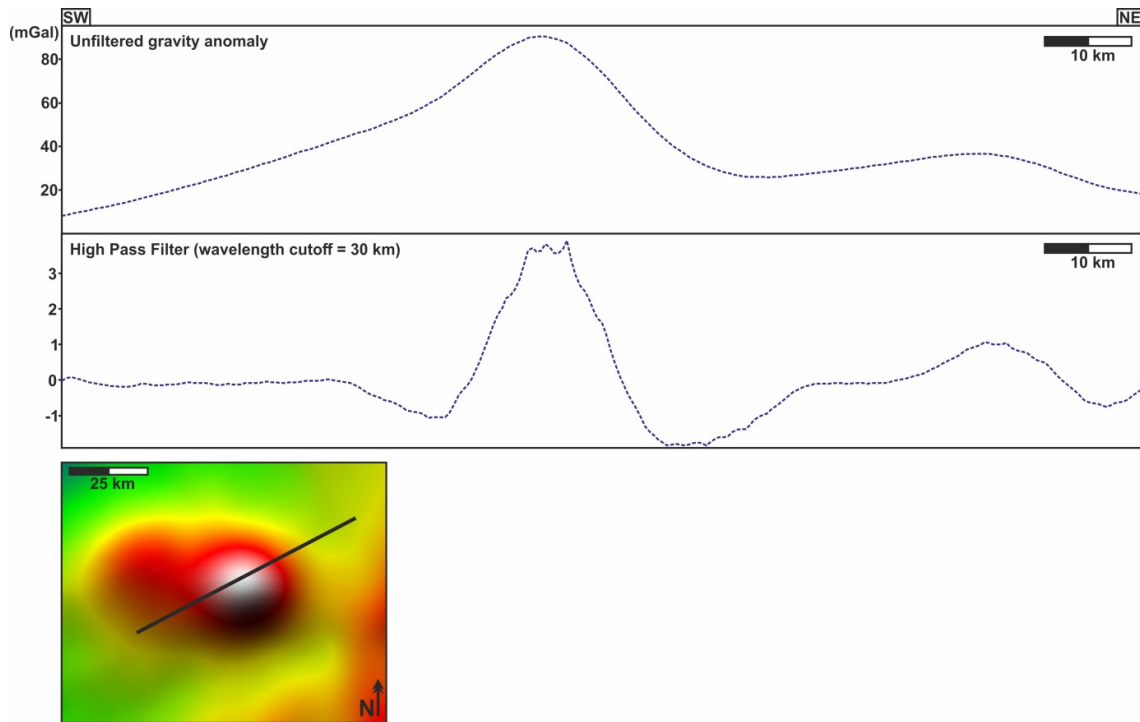


Fig. DR4: Comparison of unfiltered (top), and high-pass filtered (bottom) gravity profiles across the Erlend volcano. The wavelength cutoff is 30 km, so that the high-pass filter removes the low-frequency (i.e. wavelength > 30 km) contribution to the gravity anomaly. The presence of a positive anomaly in the high-pass profile indicates that there is a shallow, high-density body in the region of the Erlend volcano (Lowrie, 2007, p. 105-107).

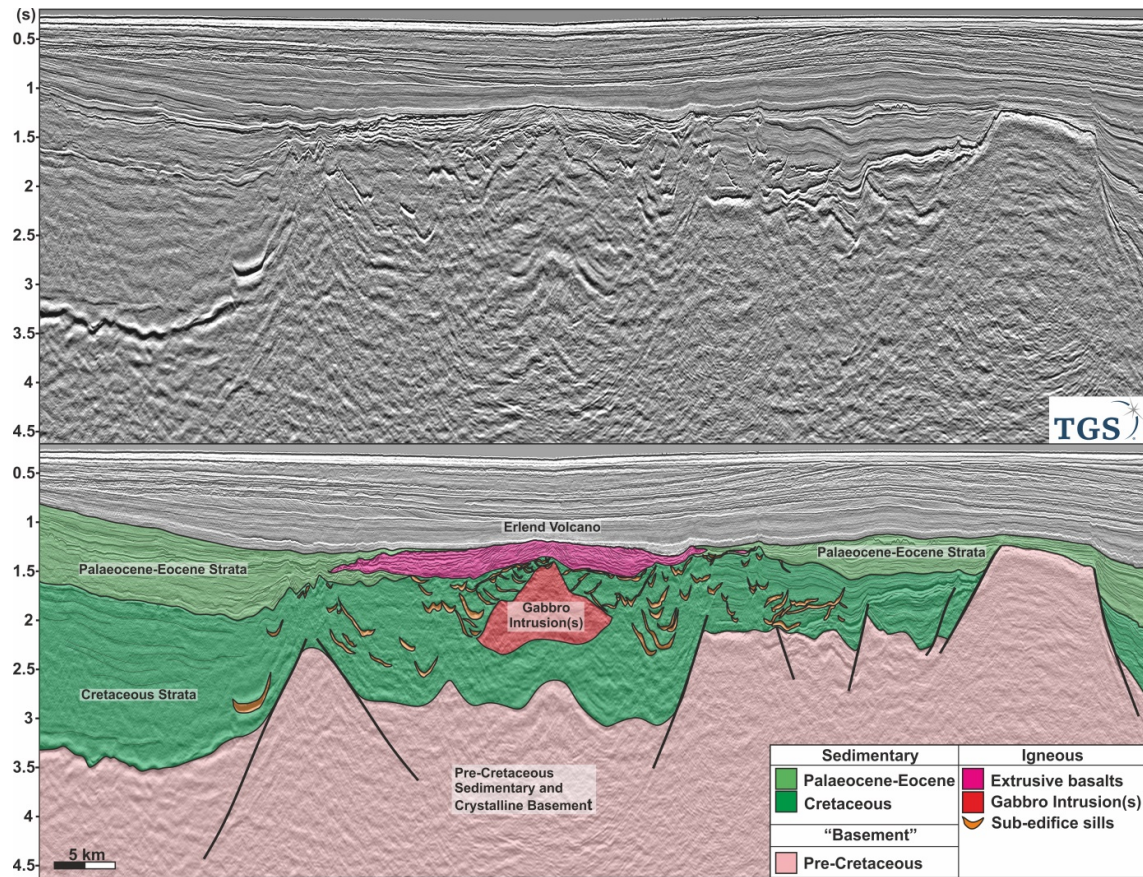


Fig. DR5: Regional seismic line showing the interpreted basement beneath and away from the Erlend volcano, showing that the high-amplitude domal reflection beneath the volcano is not the top of a basement high.

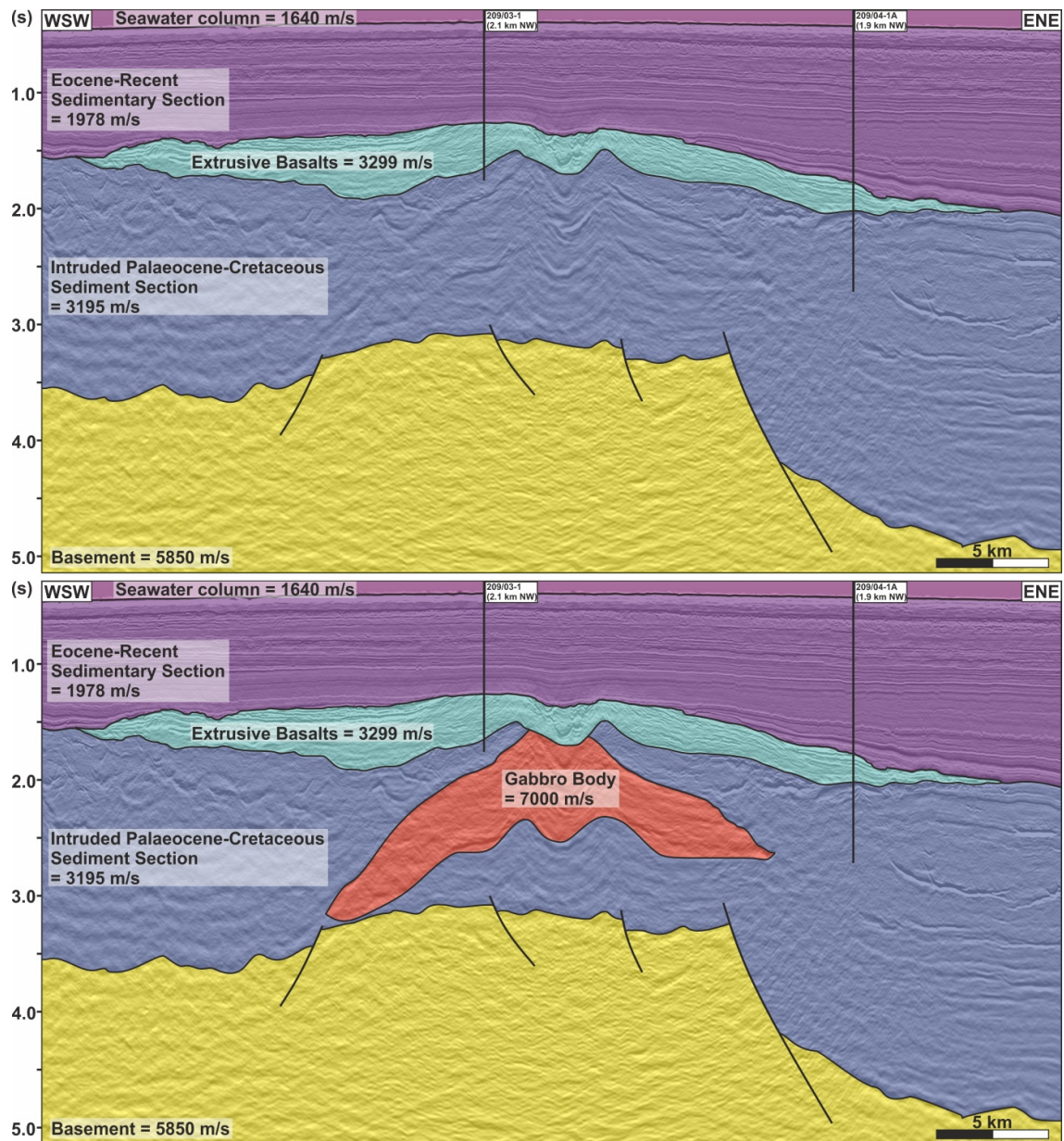


Fig. DR6: Velocity models used to depth convert the seismic line for input into the 2D gravity models. Top image shows the velocity model used for gravity Model A (ring dykes). Bottom image shows the velocity model used for gravity Models B-C.

References Cited

- Abdelmalak, M.M., Meyer, R., et al. 2016. Pre-breakup magmatism on the Voring Margin: Insight from new sub-basalt imaging and results from Ocean Drilling Program Hole 642E. *Tectonophysics*, **675**, 258–274, <https://doi.org/10.1016/j.tecto.2016.02.037>.
- Carmichael, R.S. 1989. *Practical Handbook of Physical Properties of Rocks and Minerals*. Carmichael, R. S. (ed.). CRC Press Inc.
- Christensen, N.I. & Mooney, W.D. 1995. Seismic velocity structure and composition of the continental crust: a global view. *Journal of Geophysical Research*, **100**, 9761–9788, <https://doi.org/10.1029/95JB00259>.
- Kanaris-Sotiriou, R., Morton, A.C. & Taylor, P.N. 1993. Palaeogene peraluminous magmatism, crustal melting and continental breakup: the Erlend complex, Faeroe-Shetland Basin, NE Atlantic. *Journal of the Geological Society*, **150**, 903–914, <https://doi.org/10.1144/gsjgs.150.5.0903>.
- Lowrie, W. 2007. *Fundamentals of Geophysics*, 2nd ed. Cambridge, Cambridge University Press.
- Mark, N.J., Schofield, N., et al. 2018. Igneous intrusions in the Faroe Shetland basin and their implications for hydrocarbon exploration; new insights from well and seismic data. *Marine and Petroleum Geology*, **92**, 733–753, <https://doi.org/10.1016/j.marpetgeo.2017.12.005>.
- Planke, S., Symonds, P.A., Alvestad, E. & Skogseid, J. 2000. Seismic volcanostratigraphy of large-volume basaltic extrusive complexes on rifted margins. *Journal of Geophysical Research*, **105**, 19335–19351, <https://doi.org/10.1029/1999JB900005>.
- Planke, S., Svensen, H., Myklebust, R., Bannister, S., Manton, B.M. & Lorenz, L. 2015.

Geophysics and Remote Sensing. *Advances in Volcanology*, 1–16,

<https://doi.org/10.1007/11157>.

Schofield, N., Heaton, L., Holford, S., Archer, S.G., Jackson, C.A.-L. & Jolley, D.W. 2012.

Seismic imaging of 'broken bridges': linking seismic to outcrop-scale investigations of intrusive magma lobes. *Journal of the Geological Society*, **169**, 421–426,

<https://doi.org/10.1144/0016-76492011-150>.

Schofield, N., Holford, S., et al. 2015. Regional magma plumbing and emplacement

mechanisms of the Faroe-Shetland Sill Complex: Implications for magma transport and petroleum systems within sedimentary basins. *Basin Research*, **29**, 41–63,

<https://doi.org/10.1111/bre.12164>.

Washington, H.S. 1917. *Chemical Analyses of Igneous Rocks*. United States Geological Survey,

Professional Paper 99.